ESKİŞEHİR TECHNICAL UNIVERSITY JOURNAL OF SCIENCE AND TECHNOLOGY
A- APPLIED SCIENCES AND ENGINEERING

2024, 25(1), pp. 123-140, DOI: 10.18038/estubtda.1380255

RESEACRH ARTICLE

THE NOVEL CONFORMABLE METHODS TO SOLVE CONFORMABLE TIME-FRACTIONAL COUPLED JAULENT-MIODEK SYSTEM

Özkan AVİT [1], Halil ANAÇ [2,*]

[1] Graduate Education Institute, Gumushane University, Gumushane, Turkey
[2] Torul Vocational School, Gumushane University, Gumushane, Turkey

ABSTRACT

This research utilizes two novel methods, specifically the conformable q-homotopy analysis transform method (Cq-HATM) and the conformable Elzaki Adomian decomposition method (CEADM), to examine the numerical solutions for the conformable time-fractional coupled Jaulent-Miodek system. One of the two unique methods proposed is the Cq-HATM, which is a hybrid approach that combines the q-homotopy analysis transform method with the Laplace transform, employing the concept of conformable derivative. The CEADM method, similar to the aforementioned approach, is a hybrid technique that combines the Adomian decomposition method with Elzaki transform using the concept of conformable derivative. The computer simulations were performed to offer validation for the effectiveness and dependability of the recommended approaches. After conducting a comparison between the exact solutions and the solutions acquired using the unique methods, it is apparent that both of these approaches demonstrate simplicity, effectiveness in tackling nonlinear conformable time-fractional coupled systems.

Keywords: Conformable time-fractional coupled Jaulent-Miodek system, Conformable Elzaki Adomian decomposition method, Conformable Elzaki transform

1. INTRODUCTION

The field of fractional calculus has been subject to substantial research and has been rigorously defined by a multitude of eminent scientists [1-3]. Scientists have established the essential framework for the discipline of fractional analysis. Then, the innovative conceptualizations of fractional calculus have been developed. Fractional partial differential equations are commonly utilized to develop nonlinear models and to analyse of dynamical system [4-6]. The application of fractional calculus has been employed to examine and investigate various domains, including chaos theory, financial models, disordered environments, and optics. The identification and analysis of nonlinear phenomena in the natural world are strongly dependent on the utilization of solutions derived from fractional differential equations [7-9]. A wide array of analytical and numerical approaches are utilized to get exact solutions for fractional differential equations that encompass nonlinear phenomena, owing to their intrinsic complexity [10-11].

In a recent scholarly paper, the innovative of fractional derivative and fractional integral have been presented. The authors have effectively shown that the recently introduced definition possesses the inherent attributes of the classical derivative as defined in classical analysis, while also incorporating a limit form that closely resembles the definition of the classical derivative. The author presents a new conceptualization of the fractional derivative in his scholarly contribution. The provided definition encompasses a range of mathematical ideas, such as the product rule, quotient rule, chain rule, fractional Rolle's theorem, and fractional mean value theorems. The application of the conformable fractional derivative is considered to be a fundamental and highly beneficial methodology. Moreover, it enhances our capacity to express the behavior demonstrated by concrete entities. The application of the conformable

*Corresponding Author: halilanac0638@gmail.com
Received: 23.10.2023 Published: 28.03.2024

fractional derivative represents a novel methodology for tackling complex problem domains. Fractional order models are frequently utilized in the domain of engineering and applied sciences owing to their capacity to provide a more accurate depiction of real-world occurrences. Conformable fractional derivatives have been utilized by numerous scholars from diverse academic disciplines. The application of the conformable fractional operator functions as a strategy to address certain constraints inherent in current fractional operators. The issue under consideration encompasses a collection of mathematical topics, including the mean value theorem, the chain rule, the product rule for differentiating two functions, the derivative of the quotient of two functions, and Rolle's theorem [12].

The Elzaki transform method (ETM), first proposed by Elzaki, has been employed for the resolution of linear ordinary differential equations featuring constant coefficients [13]. Elzaki utilized the differential transform method in combination with the Elzaki transform (ET) to tackle various nonlinear differential equations [14]. The Homotopy Perturbation Elzaki Transform Method (HPETM) was originally proposed by Elzaki and Hilal. In addition, HPETM has effectively resolved three nonlinear partial differential equations (PDEs) [15]. In their study, Elzaki and Kim utilized an innovative hybrid method that integrates the ET with the modified variational iteration method in order to address the radial diffusivity and shock wave equations [16-17]. In [13], Aggarwal et al. utilized ET in order to derive the solutions for linear Volterra integral equations of the first kind. However, HPETM was employed by Jena and Chakraverty in order to derive a solution for the system of time-fractional Navier-Stokes equations [18].

Nevertheless, it is crucial to acknowledge that the fractional order possesses the capacity to manifest both time and space [19-23]. The subject matter at hand concerns the progressive domain of fractional partial differential equations (FPDEs), which contain variable order fractional operators [30-31, 33]. A plethora of rigorous numerical approaches have been developed and recorded in academic literature, with significant contributions from respected scholars in the field. Numerous methods have been put up in scholarly works to address mathematical quandaries. The methods encompassed in this set of techniques consist of the Adomian Decomposition Method (ADM) [37], the Homotopy Analysis Method (HAM) [35], the Homotopy Perturbation Method (HPM) [27-29], the Collocation Method [38], the Sumudu Transform Method (STM) [36], the Differential Transformation Method (DTM) [24-25, 32, 34], and the Variational Iteration Method (VIM) [26].

The main aim of this study is to obtain novel numerical solutions for the conformable time-fractional coupled Jaulent-Miodek system using the conformable q-homotopy analysis transform method (Cq-HATM). The secondary aim of the research is to obtain novel numerical solutions for the conformable time-fractional coupled Jaulent-Miodek system with using the conformable Elzaki Adomian decomposition method (CEADM).

The following is a comprehensive list of the remaining components of the study. The fundamental principles that form the basis of conformable fractional calculus and the Elzaki transform is presented in Section 2. In Section 3, new conformable numerical methods are presented. In Section 4, an illustrated example of the conformable time-fractional coupled Jaulent-Miodek system is shown. The results are given in Section 5.

2. MATERIAL AND METHOD

This section provides some fundamental definitions.

Definition 2.1. [12, 39-41] Let a function $g: [0, \infty) \to \mathbb{R}$. Then, the conformable fractional derivative of g order α is defined as

$$T_\alpha(g)(x) = \lim_{\varepsilon \to 0} \frac{g(x + \varepsilon x^{1-\alpha}) - g(x)}{\varepsilon}, \alpha \in (0, 1]. \tag{2}$$

for all $x > 0$.

Theorem 2.1. [12, 39-41] Let $\alpha \in (0,1]$ and g, h be α −differentiable at a point $x > 0$. Then

$$(i)\ T_\alpha(ag + bh) = aT_\alpha(g) + bT_\alpha(h), \text{for all } a, b \in \mathbb{R}, \tag{3}$$

$$(ii) T_\alpha(x^p) = px^{p-1}, \text{for all } p \in \mathbb{R}, \tag{4}$$

$$(iii) T_\alpha(\lambda) = 0, for\ all\ constant\ functions, f(t) = \lambda, \tag{5}$$

$$(iv) T_\alpha(gh) = gT_\alpha(h) + hT_\alpha(g), \tag{6}$$

$$(v) T_\alpha\left(\frac{g}{h}\right) = \frac{hT_\alpha(g) - gT_\alpha(h)}{h^2}. \tag{7}$$

Definition 2.2. [42] Let $0 < \alpha \leq 1, g: [0,\infty) \to \mathbb{R}$ be function. Then, the conformable fractional Elzaki transform (CFET) of order α of g is described as

$${}_cE_\alpha[g(t)] = T_\alpha(v) = \int_0^\infty pK_\alpha(-p,t)g(t)d_\alpha t, \tag{8}$$

where $K_\alpha(-p,t) = E_\alpha\left(-\frac{1}{p}, t\right), p > 0$.

Definition 2.3. [42] Let $0 < \alpha \leq 1$, $g: [0,\infty) \to \mathbb{R}$ be real function. The CFET for the conformable fractional derivative of the function $g(t)$ is defined as

$${}_cE_\alpha[T_\alpha g(t)](p) = \frac{1}{p}\ {}_cE_\alpha[g(t)](p) - pg(0). \tag{9}$$

Definition 2.4. [45] Assume that $0 < \alpha \leq 1$, $g: [0,\infty) \to \mathbb{R}$ be real function. The conformable fractional Laplace transform of order α of g is defined by

$$\mathcal{L}_\alpha[g(t)](s) = F_\alpha(s) = \int_0^\infty E_\alpha(-s,t)g(t)d_\alpha t,$$

where E_α is Mittag-Leffler function.

2.1. The Novel Numerical Techniques

The part provides an introduction to Cq-HATM and CEADM.

2.1.1. Conformable q-homotopy analysis transform method

Now, we will present a new method. Consider the conformable time-fractional order nonlinear partial differential equation (CTFNPDE) to give the main idea of Cq-HATM:

$${}_tT_\alpha u(x,t) + Au(x,t) + Hu(x,t) = h(x,t), t > 0, n-1 < \alpha \leq n, \tag{10}$$

where A is a linear operator, H is a nonlinear operator, $h(x,t)$ is a source term, and ${}_tT_\alpha$ is a conformable fractional derivative of order α.

Now, by performing conformable Laplace transform (CLT) on Eq. (10) and using initial condition, then we get

$$s\mathcal{L}_\alpha[u(x,t)] - u(x,0) + \mathcal{L}_\alpha[Au(x,t)] + \mathcal{L}_\alpha[Hu(x,t)] = \mathcal{L}_\alpha[h(x,t)]. \tag{11}$$

If we simplify the Eq. (11), then we have

$$\mathcal{L}_\alpha[u(x,t)] - \frac{1}{s}u(x,0) + \frac{1}{s}\mathcal{L}_\alpha[Au(x,t)] + \frac{1}{s}\mathcal{L}_\alpha[Hu(x,t)] - \frac{1}{s}\mathcal{L}_\alpha[h(x,t)] = 0. \tag{12}$$

We define the nonlinear operator by the assist of HAM for real function $\varphi(x,t;q)$ as follows

$$\begin{aligned} N[\varphi(x,t;q)\,] &= \mathcal{L}_\alpha[\varphi(x,t;q)\,] - \frac{1}{s}\varphi(x,t;q)\,(0^+) + \frac{1}{s}(\mathcal{L}_\alpha[A\varphi(x,t;q)] \\ &+\mathcal{L}_\alpha[H\varphi(x,t;q)] - \mathcal{L}_\alpha[h(x,t)]), \end{aligned} \tag{13}$$

where $q\epsilon\left[0,\frac{1}{n}\right]$.

We establish a homotopy in the following:

$$(1-nq)\mathcal{L}_\alpha[\varphi(x,t;q) - u_0(x,t)] = hqH^+(x,t)H[\varphi(x,t;q)], \tag{14}$$

where, $h \neq 0$ is an auxiliary parameter and $\mathcal{L}_\alpha$ represents conformable Laplace transform. For $q = 0$ and $q = \frac{1}{n}$, the results in Eq. (14) are respectively provided:

$$\varphi(x,t;0) = u_0(x,t), \varphi\left(x,t;\frac{1}{n}\right) = u(x,t). \tag{15}$$

Therefore, by amplifying q from 0 to $\frac{1}{n}$, then the solution $\varphi(x,t;q)$ converges from $u_0(x,t)$ to the solution $u(x,t)$. Employing the Taylor theorem around q and expanding $\varphi(x,t;q)$ and then, we obtain

$$\varphi(x,t;q) = u_0(x,t) + \sum_{m=1}^{\infty} u_m(x,t)q^m, \tag{16}$$

where

$$u_m(x,t) = \frac{1}{m!}\frac{\partial^m\varphi(x,t;q)}{\partial q^m}|_{q=0}. \tag{17}$$

Eq. (16) converges at $q = \frac{1}{n}$ for the appropriate $w_0(x,t)$, n and h. Then, we have

$$u(x,t) = u_0(x,t) + \sum_{m=1}^{\infty} u_m(x,t)\left(\frac{1}{n}\right)^m. \tag{18}$$

If we differentiate the zeroth order deformation of Eq. (14) $m-$times with respect to q and we divide by $m!$, respectively, then for $q = 0$, we obtain

$$\mathcal{L}_\alpha[u_m(x,t) - k_m u_{m-1}(x,t)] = hH^+(x,t)\mathcal{R}_m(\vec{u}_{m-1}), \tag{19}$$

where the vectors are defined by

$$\vec{u}_m = \{u_0(x,t), u_1(x,t), \dots, u_m(x,t)\}. \tag{20}$$

When we apply to the inverse CLT to Eq. (19), then we obtain

$$u_m(x,t) = k_m u_{m-1}(x,t) + h\mathcal{L}_\alpha{}^{-1}[H^+(x,t)\mathcal{R}_m(\vec{u}_{m-1})], \tag{21}$$

where

$$\mathcal{R}_m(\vec{u}_{m-1}) = \mathcal{L}_\alpha[u_{m-1}(x,t)] - \left(1 - \frac{k_m}{n}\right)\frac{1}{s}u_0(x,t) + \frac{1}{s}\mathcal{L}_\alpha(Au_{m-1}(x,t) + H_{m-1}(x,t)$$

$$-h(x,t)\Big), \tag{22}$$

and

$$k_m = \begin{cases} 0, & m \le 1, \\ n, & m > 1. \end{cases} \tag{23}$$

where, H_m^+ is homotopy polynomial and presented as

$$H_m^+ = \frac{1}{m!}\frac{\partial^m \varphi(x,t;q)}{\partial q^m}|_{q=0} \quad \text{and } \varphi(x,t;q) = \varphi_0 + q\varphi_1 + q^2\varphi_2 + \cdots. \tag{24}$$

By utilizing Eqs. (21)-(22), then we obtain

$$u_m(x,t) = (k_m + h)u_{m-1}(x,t) - \left(1 - \frac{k_m}{n}\right)\frac{1}{s}u_0(x,t) + \mathrm{h}\mathcal{L}_\alpha{}^{-1}\left[\left(\frac{1}{s}\mathcal{L}_\alpha[Au_{m-1}(x,t)\right.\right.$$

$$\left.\left. + H_{m-1}(x,t) - f(x,t)]\right)\right]. \tag{25}$$

By using q-HATM, the series solution is

$$u(x,t) = \sum_{m=0}^{\infty} u_m(x,t)\left(\frac{1}{n}\right)^m. \tag{26}$$

2.1.2. Conformable Elzaki Adomian decomposition method

The examination of CTFNPDE in Eq. (10) is conducted:
Now, by performing CFET on Eq. (10) and using initial condition, then we have

$$\frac{1}{v}\ {}_cE_\alpha[u(x,t)] - vu(x,0) + \ {}_cE_\alpha[Au(x,t) + Hu(x,t)] = \ {}_cE_\alpha[h(x,t)]. \tag{27}$$

If we simplify the Eq. (27), then we get

$${}_cE_\alpha[u(x,t)] = v^2u(x,0) + v\ {}_cE_\alpha[h(x,t)] - v\ {}_cE_\alpha[Au(x,t) + Hu(x,t)]. \tag{28}$$

On applying inverse CFET to Eq. (28), then we have

$$u(x,t) = C(x,t) - \left({}_cE_\alpha\right)^{-1}\{v\ {}_cE_\alpha[Au(x,t) + Hu(x,t)]\}, \tag{29}$$

where $C(x,t)$ is obtained from initial condition and non-homogeneous term. Now, assume that, the infinite series solution is of the form:

$$u(x,t) = \sum_{m=0}^{\infty} u_m(x,t). \tag{30}$$

By employing Eqs. (29) and (30), then we have

$$\sum_{m=0}^{\infty} u_m(x,t) = C(x,t) - \left({}_cE_\alpha\right)^{-1}\left\{v\ {}_cE_\alpha\left[A\sum_{m=0}^{\infty} u_m(x,t) + \sum_{m=0}^{\infty} B_m\left(u_m(x,t)\right)\right]\right\}, \tag{31}$$

where $B_m(u_m)$ is Adomian polynomial and that denotes the nonlinear term $Hu(x,t)$. By comparing both of sides of Eq. (31), we have

$$u_0(x,t) = C(x,t), \tag{32}$$

$$u_1(x,t) = -\left({}_cE_\alpha\right)^{-1}\{v\ {}_cE_\alpha[u_0(x,t) + B_0]\}, \tag{33}$$

$$u_2(x,t) = -\left({}_cE_\alpha\right)^{-1}\{v\ {}_cE_\alpha[u_1(x,t) + B_1]\}, \tag{34}$$

⋮

In a similar manner, the general recursive relation is derived by

$$u_{m+1}(x,t) = -\left({}_cE_\alpha\right)^{-1}\{v\ {}_cE_\alpha[u_m(x,t) + B_m]\}, m \geq 1, \tag{35}$$

Ultimately, the solution $u(x,t)$ is approximated as follows.

$$u(x,t) = \sum_{m=0}^{\infty} u_m(x,t) \tag{36}$$

3. RESULTS

The part aims to present visual representations of the conformable time-fractional coupled Jaulent-Miodek system..

Example 3.1. [43-44] Consider the conformable time-fractional coupled Jaulent-Miodek system (CTFCJMS)

$$\begin{cases} u_t^\alpha + u_{xxx} + \frac{3}{2}ww_{xxx} + \frac{9}{2}w_xw_{xx} - 6uu_x - 6uww_x - \frac{3}{2}u_xw^2 = 0, \\ w_t^\alpha + w_{xxx} - 6wu_x - 6uw_x - \frac{15}{2}w_xw^2 = 0, \\ 0 < \alpha \leq 1, 0 < t \leq 1, -10 \leq x \leq 10, \end{cases} \tag{37}$$

with the initial conditions

$$u(x,0) = \frac{1}{8}\lambda^2\left(1 - 4sech^2\left(\frac{\lambda x}{2}\right)\right), \qquad w(x,0) = \lambda sech\left(\frac{\lambda x}{2}\right). \tag{38}$$

Case (i) Cq-HATM solution

CLT is employed to Eq. (37), and by applying Eq. (38), the resulting expression is produced as

$$\mathcal{L}_\alpha[u(x,t)] - \frac{u(x,0)}{s} + \frac{1}{s}\mathcal{L}_\alpha(u_{xxx} + \frac{3}{2}ww_{xxx} + \frac{9}{2}w_x.w_{xx} - 6uu_x - 6uww_x - \frac{3}{2}u_xw^2) = 0, \tag{39}$$
$$\mathcal{L}_\alpha[w] - \frac{1}{s}w(x,0) + \frac{1}{s}\mathcal{L}_\alpha\left[w_{xxx} - 6wu_x - 6uw_x - \frac{15}{2}w_xw^2\right] = 0.$$

The nonlinear operators are defined by employing Eq. (39):

$$N^1[\varphi(x,t;q),\psi(x,t;q)] = \mathcal{L}_\alpha[\varphi(x,t;q)] - \frac{1}{s}\left(\frac{1}{8}\lambda^2\left(1 - 4sech^2\left(\frac{\lambda x}{2}\right)\right)\right) + \frac{1}{s}\mathcal{L}_\alpha\left[\frac{\partial^3\varphi}{\partial x^3} + \frac{3}{2}\psi\frac{\partial^3\psi}{\partial x^3} + \frac{9}{2}\frac{\partial\psi}{\partial x}.\frac{\partial^2\psi}{\partial x^2} - 6\varphi\frac{\partial\varphi}{\partial x} - 6\varphi\psi\frac{\partial\psi}{\partial x} - \frac{3}{2}\frac{\partial\varphi}{\partial x}\psi^2\right] \tag{40}$$

$$N^2[\varphi(x,t;q),\psi(x,t;q)] = \mathcal{L}_\alpha[\psi(x,t;q)] - \frac{1}{s}\left(\lambda sech\left(\frac{\lambda x}{2}\right)\right) + \frac{1}{s}\mathcal{L}_\alpha\left[\frac{\partial^3\psi}{\partial x^3} - 6\psi\frac{\partial\varphi}{\partial x} - 6\varphi\frac{\partial\psi}{\partial x} - \frac{15}{2}\psi^2\frac{\partial\psi}{\partial x}\right]. \tag{41}$$

The $m-th$ order deformation equations are defined by the application of the proposed algorithm:

$$\mathcal{L}_\alpha[u_m(x,t) - k_mu_{m-1}(x,t)] = h\mathcal{R}_{1,m}[\vec{u}_{m-1},\vec{w}_{m-1}], \tag{42}$$

$$\mathcal{L}_\alpha[w_m(x,t) - k_mw_{m-1}(x,t)] = h\mathcal{R}_{2,m}[\vec{u}_{m-1},\vec{w}_{m-1}], \tag{43}$$

where

$$\mathcal{R}_{1,m}[\vec{u}_{m-1},\vec{w}_{m-1}] = \mathcal{L}_\alpha[u_{m-1}] - \frac{1}{s}(1 - \frac{km}{n})(\frac{1}{8}\lambda^2\left(1 - 4sech^2\left(\frac{\lambda x}{2}\right)\right) + \frac{1}{s}\mathcal{L}_\alpha\left[\frac{\partial^3u_{m-1}}{\partial x^3} + \frac{3}{2}\sum_{r=0}^{m-1}w_r\frac{\partial^3w_{m-1-r}}{\partial x^3} + \frac{9}{2}\sum_{r=0}^{m-1}\frac{\partial w_r}{\partial x}\frac{\partial^2w_{m-1-r}}{\partial x^2} - 6\sum_{r=0}^{m-1}u_r\frac{\partial u_{m-1-r}}{\partial x} - 6\sum_{r=0}^{m-1}\left(\sum_{j=0}^{r}u_jw_{r-j}\right)\frac{\partial w_{m-1-r}}{\partial x} - \frac{3}{2}\sum_{r=0}^{m-1}\left(\sum_{j=0}^{r}w_jw_{r-j}\right)\frac{\partial w_{m-1-r}}{\partial x}\right], \tag{44}$$

$$\mathcal{R}_{2,m}[\vec{u}_{m-1},\vec{w}_{m-1}] = \mathcal{L}_\alpha[w_{m-1}] - \frac{1}{s}\left(1-\frac{km}{n}\right)\left(\lambda sech\left(\frac{\lambda x}{2}\right)\right) + \frac{1}{s}\mathcal{L}_\alpha\left[\frac{\partial^3 u_{m-r}}{\partial x^3} - 6\sum_{r=0}^{m-1} w_r \frac{\partial u_{m-1-r}}{\partial x} - 6\sum_{r=0}^{m-1} u_r \frac{\partial w_{m-1-r}}{\partial x} - \frac{15}{2}\sum_{r=0}^{m-1}\left(\sum_{j=0}^{r} w_j w_{r-j}\right)\frac{\partial w_{m-1-r}}{\partial x}\right]. \quad (45)$$

By utilizing the inverse CLT to Eqs. (42)-(43), we obtain

$$u_m(x,t) = k_m u_{m-1}(x,t) + h\mathcal{L}_\alpha{}^{-1}\{\mathcal{R}_{1,m}[\vec{u}_{m-1},\vec{w}_{m-1}]\}, \quad (46)$$

$$w_m(x,t) = k_m w_{m-1}(x,t) + h\mathcal{L}_\alpha{}^{-1}\{\mathcal{R}_{2,m}[\vec{u}_{m-1},\vec{w}_{m-1}]\}. \quad (47)$$

By employing initial conditions, we are able to drive

$$u_0(x,t) = \frac{1}{8}\lambda^2\left(1-4sech^2\left(\frac{\lambda x}{2}\right)\right), \quad (48)$$

$$w_0(x,t) = \lambda sech\left(\frac{\lambda x}{2}\right). \quad (49)$$

To get the values of $u_1(x,t)$ and $w_1(x,t)$, we substitute $m=1$ into Eqs. (46)-(47), resulting in the following expressions:

$$u_1(x,t) = -h\frac{\sinh\left(\frac{\lambda x}{2}\right)\lambda^5 t^\alpha}{4\alpha cosh^3(\frac{\lambda x}{2})}, \quad (50)$$

$$w_1(x,t) = h\frac{t^\alpha\lambda^4\sinh\left(\frac{\lambda x}{2}\right)}{4\alpha\cosh^2\left(\frac{\lambda x}{2}\right)}. \quad (51)$$

In a similar vein, by substituting $m=2$ into Eqs. (46)-(47), the resulting values for $u_2(x,t)$ and $w_2(x,t)$ can be obtained:

$$u_2(x,t) = -(n+h)h\frac{t^\alpha\lambda^5\sinh\left(\frac{\lambda x}{2}\right)}{4\alpha\cosh^3\left(\frac{\lambda x}{2}\right)} - h^2\left(\frac{t^{2\alpha}\lambda^8\left(\cosh^2\left(\frac{\lambda x}{2}\right)-\frac{3}{2}\right)}{16\alpha^2\cosh^4\left(\frac{\lambda x}{2}\right)}\right), \quad (52)$$

$$w_2(x,t) = (n+h)h\frac{t^\alpha\lambda^4\sinh\left(\frac{\lambda x}{2}\right)}{4\alpha\cosh^2\left(\frac{\lambda x}{2}\right)} + h^2\left(\frac{t^{2\alpha}\lambda^7\left(\cosh^2\left(\frac{\lambda x}{2}\right)-2\right)}{32\alpha^2\cosh^3\left(\frac{\lambda x}{2}\right)}\right). \quad (53)$$

By employing this approach, it is possible to identify the remaining terms. The solutions of the CTFCJMS are determined through the Cq-HATM:

$$u(x,t) = u_0(x,t) + \sum_{m=1}^{\infty} u_m(x,t)\left(\frac{1}{n}\right)^m, \tag{54}$$

$$w(x,t) = w_0(x,t) + \sum_{m=1}^{\infty} w_m(x,t)\left(\frac{1}{n}\right)^m. \tag{55}$$

By substituting $\alpha = 1, n = 1,\ h = -1$ into Eqs. (54)-(55), we have that the resulting outcomes, denoted as $\sum_{m=1}^{M} u_m(x,t)\left(\frac{1}{n}\right)^m$ and $\sum_{m=1}^{M} w_m(x,t)\left(\frac{1}{n}\right)^m$, respectively, converge to the exact solutions $u(x,t) = \xi - \kappa\coth[\kappa(x+\theta-\xi t)]$ and $w(x,t) = -\kappa^2\operatorname{cosech}^2[\kappa(x+\theta-\xi t)]$ of the CTFCJMS when $M \to \infty$.

Case (ii) CEADM solution

By employing the CFET to Eq. (37) and utilizing Eq. (38), the resulting expression is obtained.

$$\begin{aligned}\frac{1}{v}E_\alpha^c\{u(x,t)\} - vu(x,0) \\ + E_\alpha^c\left[\frac{\partial^3 u}{\partial x^3} + \frac{3}{2}w\frac{\partial^3 w}{\partial x^3} + \frac{9}{2}\frac{\partial w}{\partial x}\frac{\partial^2 w}{\partial x^2} - 6u\frac{\partial u}{\partial x} - 6uw\frac{\partial w}{\partial x} - \frac{3}{2}\frac{\partial u}{\partial x}w^2\right] = 0,\end{aligned} \tag{56}$$

$$\frac{1}{v}E_\alpha^c\{w(x,t)\} - vw(x,0) + E_\alpha^c\left[\frac{\partial^3 w}{\partial x^3} - 6w\frac{\partial u}{\partial x} - 6u\frac{\partial w}{\partial x} - \frac{15}{2}\frac{\partial w}{\partial x}w^2\right] = 0. \tag{57}$$

Rearranging Eqs. (56)-(57), then we obtain

$$\begin{aligned}E_\alpha^c\{u(x,t)\} = v^2\,u(x,0) \\ - vE_\alpha^c\left[\frac{\partial^3 u}{\partial x^3} + \frac{3}{2}w\frac{\partial^3 w}{\partial x^3} + \frac{9}{2}\frac{\partial w}{\partial x}\frac{\partial^2 w}{\partial x^2} - 6u\frac{\partial u}{\partial x} - 6uw\frac{\partial w}{\partial x} - \frac{3}{2}\frac{\partial u}{\partial x}w^2\right],\end{aligned} \tag{58}$$

$$E_\alpha^c\{w(x,t)\} = v^2\,w(x,0) - vE_\alpha^c\left[\frac{\partial^3 w}{\partial x^3} - 6w\frac{\partial u}{\partial x} - 6u\frac{\partial w}{\partial x} - \frac{15}{2}\frac{\partial w}{\partial x}w^2\right]. \tag{59}$$

By utilizing the inverse CFET on Eqs. (58)-(59), we are able to derive the following result:

$$\begin{aligned}u(x,t) = \frac{1}{8}\lambda^2\left(1 - 4\operatorname{sech}^2\left[\frac{\lambda x}{2}\right]\right) - (E_\alpha^c)^{-1}\{vE_\alpha^c\left[\frac{\partial^3 u}{\partial x^3} + \frac{3}{2}w\frac{\partial^3 w}{\partial x^3} + \frac{9}{2}\frac{\partial w}{\partial x}\frac{\partial^2 w}{\partial x^2} - 6u\frac{\partial u}{\partial x}\right. \\ \left. -6uw\frac{\partial w}{\partial x} - \frac{3}{2}\frac{\partial u}{\partial x}w^2\right]\},\end{aligned} \tag{60}$$

$$w(x,t) = \lambda\operatorname{sech}\left[\frac{\lambda x}{2}\right] - (E_\alpha^c)^{-1}\left\{vE_\alpha^c\left[\frac{\partial^3 w}{\partial x^3} - 6w\frac{\partial u}{\partial x} - 6u\frac{\partial w}{\partial x} - \frac{15}{2}\frac{\partial w}{\partial x}w^2\right]\right. . \tag{61}$$

Let us consider the assumption that the answer to the infinite series can be expressed in the following form:

$$u(x,t) = \sum_{m=0}^{\infty} u_m(x,t), \tag{62}$$

$$w(x,t)=\sum_{m=0}^{\infty} w_m(x,t). \tag{63}$$

Utilizing Adomian decomposition method, if we rewrite Eqs. (62)-(63), then it is obtained as

$$\sum_{m=0}^{\infty} u_m(x,t)=\frac{1}{8}\lambda^2\left(1-4\operatorname{sech}^2\left[\frac{\lambda x}{2}\right]\right)-(E_\alpha^c)^{-1}\left\{vE_\alpha^c\left[\frac{\partial^3 u_{m-1}(x,t)}{\partial x^3}+\frac{3}{2}\sum_{m=0}^{\infty}A_m+\frac{9}{2}\sum_{m=0}^{\infty}B_m-6\sum_{m=0}^{\infty}C_m-6\sum_{m=0}^{\infty}E_m-\frac{3}{2}\sum_{m=0}^{\infty}F_m\right]\right\}, \tag{64}$$

$$\sum_{m=0}^{\infty} w_m(x,t)=\lambda\operatorname{sech}\left[\frac{\lambda x}{2}\right]-(E_\alpha^c)^{-1}\left\{vE_\alpha^c\left[\frac{\partial^3 w_{m-1}(x,t)}{\partial x^3}-6\sum_{m=0}^{\infty}G_m-6\sum_{m=0}^{\infty}H_m-\frac{15}{2}\sum_{m=0}^{\infty}K_m\right]\right\}, \tag{65}$$

where $A_m, B_m, C_m, E_m, F_m, G_m, H_m, K_m$ are Adomian polynomials of the form $w\frac{\partial^3 w}{\partial x^3}=\sum_{m=0}^{\infty}A_m$, $\frac{\partial w}{\partial x}\frac{\partial^2 w}{\partial x^2}=\sum_{m=0}^{\infty}B_m$, $u\frac{\partial u}{\partial x}=\sum_{m=0}^{\infty}C_m$, $uw\frac{\partial w}{\partial x}=\sum_{m=0}^{\infty}E_m$, $w^2\frac{\partial u}{\partial x}=\sum_{m=0}^{\infty}F_m$, $w\frac{\partial w}{\partial x}=\sum_{m=0}^{\infty}G_m$, $u\frac{\partial w}{\partial x}=\sum_{m=0}^{\infty}H_m$, $w^2\frac{\partial w}{\partial x}=\sum_{m=0}^{\infty}K_m$.

By taking both sides of Eqs. (64)-(65) and making use of the initial condition (38) and Eqs. (64)-(65), we simply obtain the following iterations:

$$u_0(x,t)=\frac{1}{8}\lambda^2\left(1-4\operatorname{sech}^2\left[\frac{\lambda x}{2}\right]\right), \tag{66}$$

$$w_0(x,t)=\lambda\operatorname{sech}\left[\frac{\lambda x}{2}\right], \tag{67}$$

$$u_1(x,t)=\frac{t^\alpha\lambda^5\sinh\left(\frac{\lambda x}{2}\right)}{4\alpha\cosh^3\left(\frac{\lambda x}{2}\right)}, \tag{68}$$

$$w_1(x,t)=-\frac{t^\alpha\lambda^4\sinh\left(\frac{\lambda x}{2}\right)}{4\alpha\cosh^2\left(\frac{\lambda x}{2}\right)}, \tag{69}$$

$$u_2(x,t)=-\left(\frac{t^{2\alpha}\lambda^8\left(2\cosh^2\left(\frac{\lambda x}{2}\right)-3\right)}{32\alpha^2\cosh^4\left(\frac{\lambda x}{2}\right)}\right), \tag{68}$$

$$w_2(x,t)=\left(\frac{t^{2\alpha}\lambda^7\left(\cosh^2\left(\frac{\lambda x}{2}\right)-2\right)}{32\alpha^2\cosh^3\left(\frac{\lambda x}{2}\right)}\right). \tag{69}$$

By continuing in a similar manner, the outcomes for CTFCJMS can be derived.

$$u(x,t) = \sum_{m=0}^{\infty} u_m(x,t) = u_0(x,t) + u_1(x,t) + u_2(x,t) + \cdots$$

$$= \frac{1}{8}\lambda^2\left(1 - 4\text{sech}^2\left[\frac{\lambda x}{2}\right]\right) + \frac{t^{\alpha}\lambda^5 \sinh\left(\frac{\lambda x}{2}\right)}{4\alpha\cosh^3\left(\frac{\lambda x}{2}\right)} - \left(\frac{t^{2\alpha}\lambda^8\left(2\cosh^2\left(\frac{\lambda x}{2}\right) - 3\right)}{32\alpha^2\cosh^4\left(\frac{\lambda x}{2}\right)}\right), \tag{70}$$

$$w(x,t) = \sum_{m=0}^{\infty} w_m(x,t) = w_0(x,t) + w_1(x,t) + w_2(x,t) + \cdots$$

$$= \lambda\text{sech}\left[\frac{\lambda x}{2}\right] - \frac{t^{\alpha}\lambda^4 \sinh\left(\frac{\lambda x}{2}\right)}{4\alpha\cosh^2\left(\frac{\lambda x}{2}\right)} + \left(\frac{t^{2\alpha}\lambda^7\left(\cosh^2\left(\frac{\lambda x}{2}\right) - 2\right)}{32\alpha^2\cosh^3\left(\frac{\lambda x}{2}\right)}\right). \tag{71}$$

Figure 1 displays the 3D graphical representations of Cq-HATM, the exact solution, and the absolute error for $u(x,t)$ and $w(x,t)$.

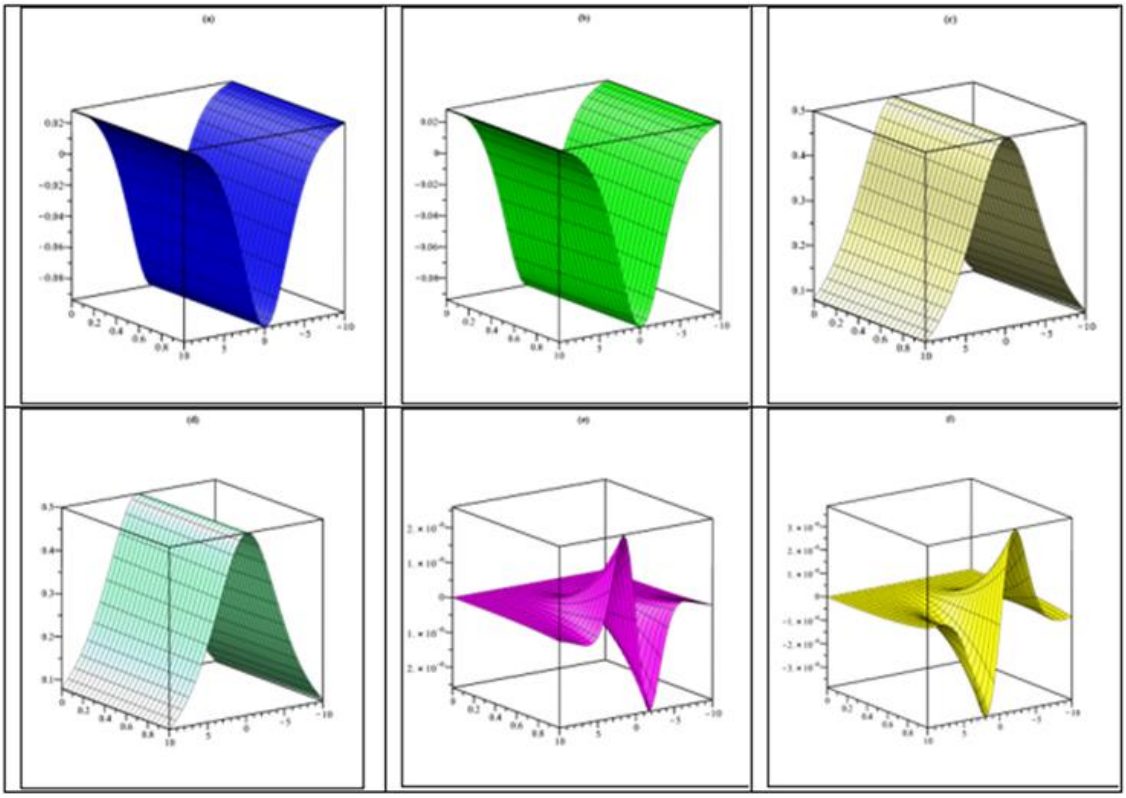

Figure 1. (a) Nature of Cq-HATM solution $u(x,t)$ **(b)** Nature of exact solution $u(x,t)$ **(c)** Nature of Cq-HATM solution $w(x,t)$ **(d)** Nature of exact solution $w(x,t)$ **(e)** Nature of absolute error=$\left|u_{exact} - u_{Cq-HATM}\right|$ **(f)** Nature of absolute error=$\left|w_{exact} - w_{Cq-MHATM}\right|$ at $\lambda = 0.5, h = -1, n = 1, \alpha = 1$ for Ex. 3.1.

Figure 2 presents the three-dimensional graphical depictions of CEADM, the exact solution, and the absolute error for $u(x,t)$ and $w(x,t)$.

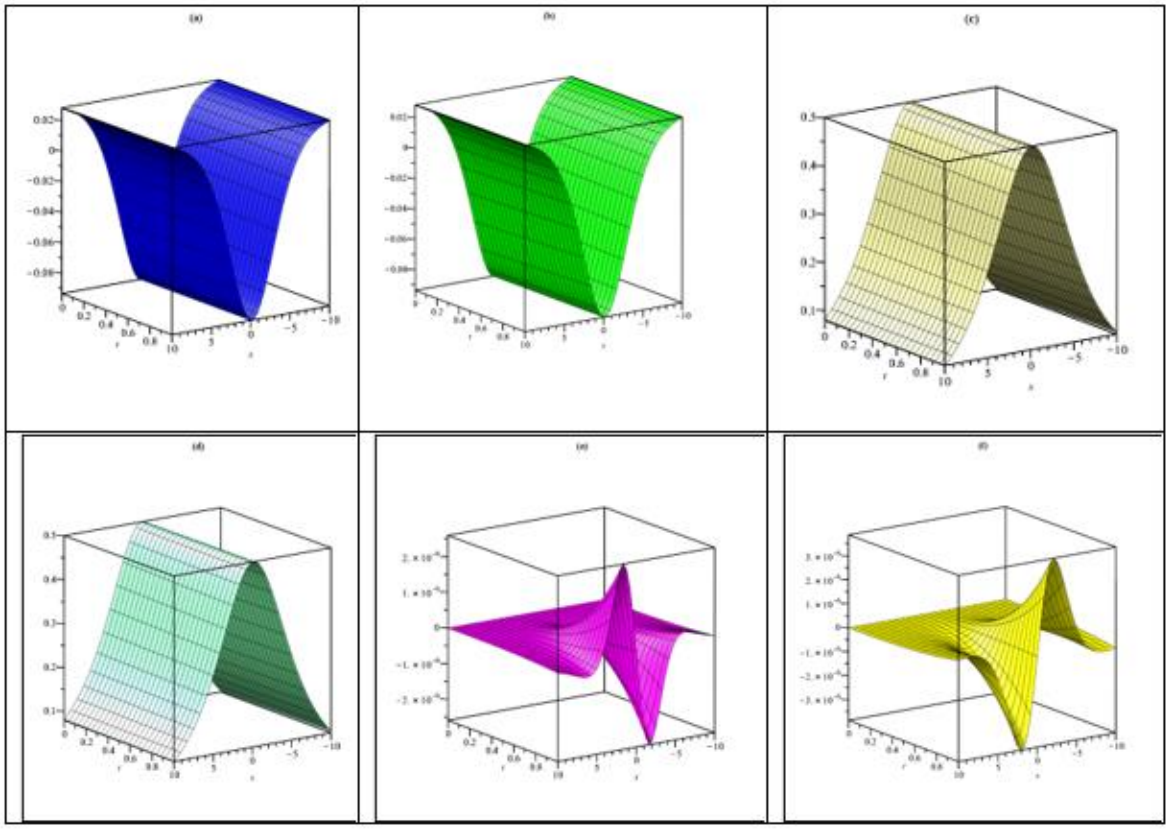

Figure 2. (a) Nature of CEADM solution $u(x,t)$ **(b)** Nature of exact solution $u(x,t)$ **(c)** Nature of CEADM solution $w(x,t)$ **(d)** Nature of exact solution $w(x,t)$ **(e)** Nature of absolute error=$|u_{exact} - u_{\text{CEADM}}|$ **(f)** Nature of absolute error=$|w_{exact} - w_{\text{CEADM}}|$ at $\lambda = 0.5, \alpha = 1$ for Ex. 3.1.

Figure 3 shows the two-dimensional graphical representations of Cq-HATM for $u(x,t), w(x,t)$ solutions and the exact solution for different α values.

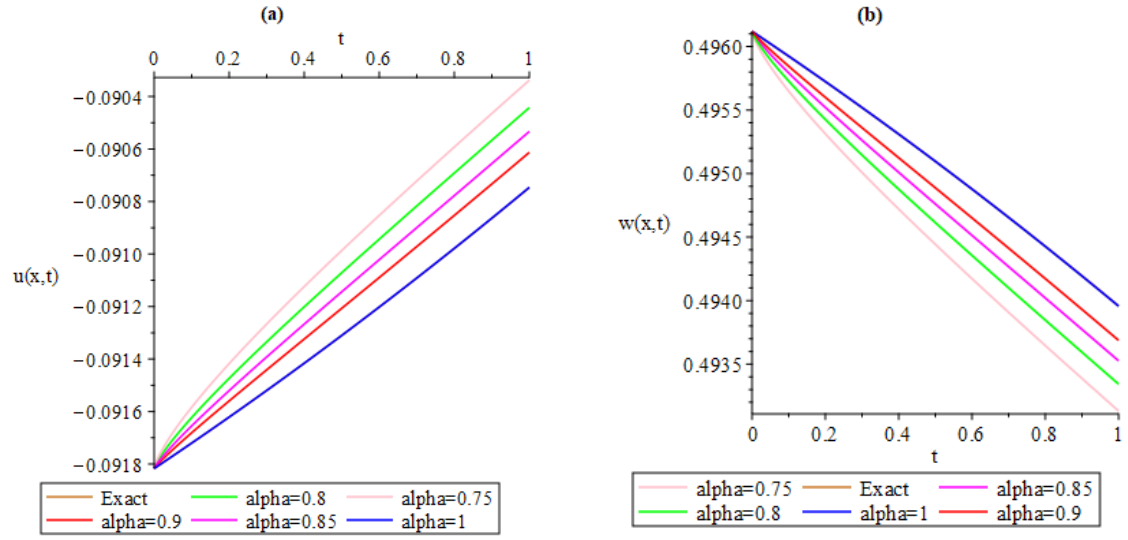

Figure 3. The comparison of the Cq-HATM solutions for $u(x,t)$ and exact solution **(b)** The comparison of the Cq-HATM solutions for $w(x,t)$ and exact solution at $\lambda = 0.5, h = -1, n = 1, x = 0.5$ with different α.

Figure 4 displays the graphical depictions of CEADM for the solutions $u(x,t)$ and $w(x,t)$, as well as the exact solution, in a two-dimensional format. These representations vary based on the different α values.

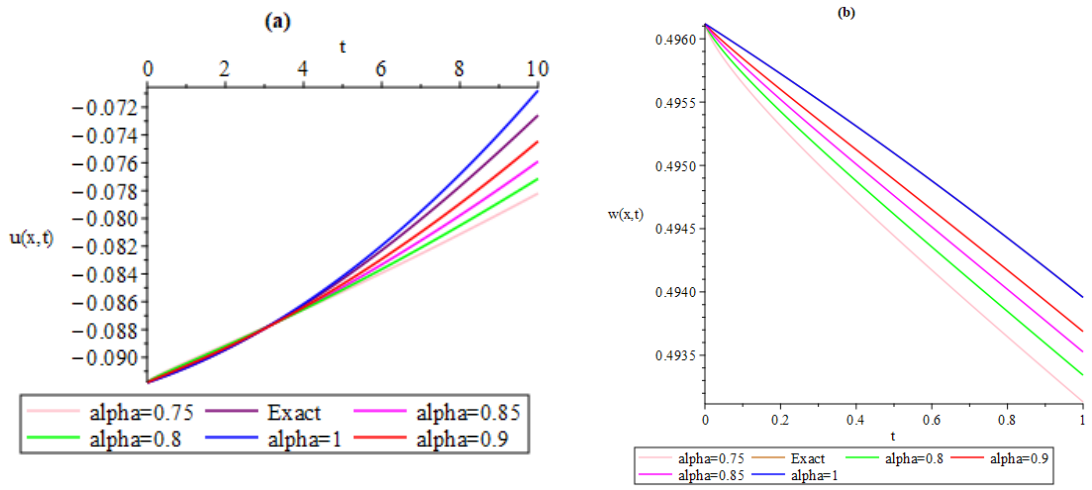

Figure 4. The comparison of the CEADM solutions for $u(x,t)$ and exact solution **(b)** The comparison of the CEADM solutions s for $w(x,t)$ and exact solution at $\lambda = 0.5, x = 0.5$ with different α.

Table 1 shows the numerical solution of $u(x,t)$ obtained from the solution of CTFCJMS with Cq-HATM for different x, t and α values.

Table 1. Numerical solution of $u(x,t)$ by Cq-HATM for CTFCJMS with different x, t and α at $\lambda = 0.5, n = 1, h = -1$.

x	t	$\alpha = 0.75$	$\alpha = 0.80$	$\alpha = 0.85$	$\alpha = 0.90$	$\alpha = 1$
0.1	0.001	1.2×10^{-6}	7.7×10^{-7}	4.5×10^{-7}	2.3×10^{-7}	2.5×10^{-16}
	0.002	2.0×10^{-6}	1.3×10^{-6}	7.7×10^{-7}	4.1×10^{-7}	2.0×10^{-15}
	0.003	2.7×10^{-6}	1.7×10^{-6}	1.0×10^{-6}	5.8×10^{-7}	6.8×10^{-15}
	0.004	3.4×10^{-6}	2.1×10^{-6}	1.3×10^{-6}	7.3×10^{-7}	1.6×10^{-14}
	0.005	3.9×10^{-6}	2.5×10^{-6}	1.5×10^{-6}	8.7×10^{-7}	3.1×10^{-14}
0.2	0.001	2.5×10^{-6}	1.5×10^{-6}	9.0×10^{-7}	4.7×10^{-7}	5.0×10^{-16}
	0.002	4.1×10^{-6}	2.6×10^{-6}	1.5×10^{-6}	8.3×10^{-7}	4.0×10^{-15}
	0.003	5.5×10^{-6}	3.5×10^{-6}	2.1×10^{-6}	1.1×10^{-6}	1.3×10^{-14}
	0.004	6.7×10^{-6}	4.3×10^{-6}	2.6×10^{-6}	1.4×10^{-6}	3.2×10^{-14}
	0.005	7.8×10^{-6}	5.1×10^{-6}	3.1×10^{-6}	1.7×10^{-6}	6.3×10^{-14}
0.3	0.001	3.7×10^{-6}	2.3×10^{-6}	1.3×10^{-6}	7.0×10^{-7}	7.5×10^{-16}
	0.002	6.1×10^{-6}	3.8×10^{-6}	2.3×10^{-6}	1.2×10^{-6}	6.0×10^{-15}
	0.003	8.2×10^{-6}	5.2×10^{-6}	3.1×10^{-6}	1.7×10^{-6}	2.0×10^{-14}
	0.004	1.0×10^{-5}	6.4×10^{-6}	3.9×10^{-6}	2.1×10^{-6}	4.8×10^{-14}
	0.005	1.1×10^{-5}	7.6×10^{-6}	4.6×10^{-6}	2.5×10^{-6}	9.3×10^{-14}
0.4	0.001	5.0×10^{-6}	3.0×10^{-6}	1.7×10^{-6}	9.3×10^{-7}	9.8×10^{-16}
	0.002	8.1×10^{-6}	5.1×10^{-6}	3.0×10^{-6}	1.6×10^{-6}	7.9×10^{-15}
	0.003	1.0×10^{-5}	6.9×10^{-6}	4.1×10^{-6}	2.2×10^{-6}	2.6×10^{-14}
	0.004	1.3×10^{-5}	8.5×10^{-6}	5.2×10^{-6}	2.8×10^{-6}	6.3×10^{-14}
	0.005	1.5×10^{-5}	1.0×10^{-5}	6.2×10^{-6}	3.4×10^{-6}	1.2×10^{-13}
0.5	0.001	6.2×10^{-6}	3.8×10^{-6}	2.2×10^{-6}	1.1×10^{-6}	1.2×10^{-15}
	0.002	1.0×10^{-5}	6.3×10^{-6}	3.8×10^{-6}	2.0×10^{-6}	9.7×10^{-15}
	0.003	1.3×10^{-5}	8.6×10^{-6}	5.2×10^{-6}	2.8×10^{-6}	3.2×10^{-14}
	0.004	1.6×10^{-5}	1.0×10^{-5}	6.4×10^{-6}	3.5×10^{-6}	7.7×10^{-14}
	0.005	1.9×10^{-5}	1.2×10^{-5}	7.6×10^{-6}	4.2×10^{-6}	1.5×10^{-13}

Table 2 presents the numerical solution of the function $w(x,t)$, which was derived from the solution of the CTFCJMS using the Cq-HATM. The table displays the results for various values of x, t, and α.

Table 2. Numerical solution of $w(x,t)$ by Cq-HATM for CTFCJMS with different x, t and α at $\lambda = 0.5, n = 1, h = -1$.

x	t	$\alpha = 0.75$	$\alpha = 0.80$	$\alpha = 0.85$	$\alpha = 0.90$	$\alpha = 1$
0.1	0.001	2.5×10^{-6}	1.5×10^{-6}	9.0×10^{-7}	4.7×10^{-7}	3.1×10^{-16}
	0.002	4.1×10^{-6}	2.6×10^{-6}	1.5×10^{-6}	8.3×10^{-7}	2.5×10^{-15}
	0.003	5.5×10^{-6}	3.5×10^{-6}	2.1×10^{-6}	1.1×10^{-6}	8.5×10^{-15}
	0.004	6.8×10^{-6}	4.3×10^{-6}	2.6×10^{-6}	1.4×10^{-6}	2.0×10^{-14}
	0.005	7.9×10^{-6}	5.1×10^{-6}	3.1×10^{-6}	1.7×10^{-6}	3.9×10^{-14}
0.2	0.001	5.0×10^{-6}	3.1×10^{-6}	1.8×10^{-6}	9.4×10^{-7}	6.3×10^{-16}
	0.002	8.3×10^{-6}	5.2×10^{-6}	3.1×10^{-6}	1.6×10^{-6}	5.0×10^{-15}
	0.003	1.1×10^{-5}	7.0×10^{-6}	4.2×10^{-6}	2.3×10^{-6}	1.7×10^{-14}
	0.004	1.3×10^{-5}	8.6×10^{-6}	5.3×10^{-6}	2.9×10^{-6}	4.0×10^{-14}
	0.005	1.5×10^{-5}	1.0×10^{-5}	6.2×10^{-6}	3.4×10^{-6}	7.9×10^{-14}
0.3	0.001	7.5×10^{-6}	4.6×10^{-6}	2.7×10^{-6}	1.4×10^{-6}	9.4×10^{-16}
	0.002	1.2×10^{-5}	7.7×10^{-6}	4.6×10^{-6}	2.4×10^{-6}	7.5×10^{-15}
	0.003	1.6×10^{-5}	1.0×10^{-5}	6.3×10^{-6}	3.4×10^{-6}	2.5×10^{-14}
	0.004	2.0×10^{-5}	1.2×10^{-5}	7.9×10^{-6}	4.3×10^{-6}	6.0×10^{-14}
	0.005	2.3×10^{-5}	1.5×10^{-5}	9.3×10^{-6}	5.1×10^{-6}	1.1×10^{-13}
0.4	0.001	1.0×10^{-5}	6.1×10^{-6}	3.5×10^{-6}	1.8×10^{-6}	1.2×10^{-15}
	0.002	1.6×10^{-5}	1.0×10^{-5}	6.1×10^{-6}	3.3×10^{-6}	9.9×10^{-15}
	0.003	2.1×10^{-5}	1.3×10^{-5}	8.4×10^{-6}	4.5×10^{-6}	3.3×10^{-14}
	0.004	2.6×10^{-5}	1.7×10^{-5}	1.0×10^{-5}	5.7×10^{-6}	7.9×10^{-14}
	0.005	3.1×10^{-5}	2.0×10^{-5}	1.2×10^{-5}	6.8×10^{-6}	1.5×10^{-13}
0.5	0.001	1.2×10^{-5}	7.6×10^{-6}	4.4×10^{-6}	2.3×10^{-6}	1.5×10^{-15}
	0.002	2.0×10^{-5}	1.2×10^{-5}	7.6×10^{-5}	4.1×10^{-6}	1.2×10^{-14}
	0.003	2.7×10^{-5}	1.7×10^{-5}	1.0×10^{-5}	5.7×10^{-6}	4.1×10^{-14}
	0.004	3.3×10^{-5}	2.1×10^{-5}	1.3×10^{-5}	7.1×10^{-6}	9.8×10^{-14}
	0.005	3.8×10^{-5}	2.5×10^{-5}	1.5×10^{-5}	8.5×10^{-6}	1.9×10^{-13}

Table 3 demonstrates the numerical solution of $u(x,t)$ obtained from the solution of CTFCJMS with CEADM for distinct x, t and α values.

Table 3. Numerical solution of $u(x,t)$ by CEADM for CTFCJMS with different x, t and α at $\lambda = 0.5$.

x	t	$\alpha = 0.75$	$\alpha = 0.80$	$\alpha = 0.85$	$\alpha = 0.90$	$\alpha = 1$
0.1	0.001	1.2×10^{-6}	7.7×10^{-7}	4.5×10^{-7}	2.3×10^{-7}	2.5×10^{-16}
	0.002	2.0×10^{-6}	1.3×10^{-6}	7.7×10^{-7}	4.1×10^{-7}	2.0×10^{-15}
	0.003	2.7×10^{-6}	1.7×10^{-6}	1.0×10^{-6}	5.8×10^{-7}	6.8×10^{-15}
	0.004	3.4×10^{-6}	2.1×10^{-6}	1.3×10^{-6}	7.3×10^{-7}	1.6×10^{-14}
	0.005	3.9×10^{-6}	2.5×10^{-6}	1.5×10^{-6}	8.7×10^{-7}	3.1×10^{-14}
0.2	0.001	2.5×10^{-6}	1.5×10^{-6}	9.0×10^{-7}	4.7×10^{-7}	5.0×10^{-16}
	0.002	4.1×10^{-6}	2.6×10^{-6}	1.5×10^{-6}	8.3×10^{-7}	4.0×10^{-15}
	0.003	5.5×10^{-6}	3.5×10^{-6}	2.1×10^{-6}	1.1×10^{-6}	1.3×10^{-14}
	0.004	6.7×10^{-6}	4.3×10^{-6}	2.6×10^{-6}	1.4×10^{-6}	3.2×10^{-14}
	0.005	7.8×10^{-6}	5.1×10^{-6}	3.1×10^{-6}	1.7×10^{-6}	6.3×10^{-14}
0.3	0.001	3.7×10^{-6}	2.3×10^{-6}	1.3×10^{-6}	7.0×10^{-7}	7.5×10^{-16}
	0.002	6.1×10^{-6}	3.8×10^{-6}	2.3×10^{-6}	1.2×10^{-6}	6.0×10^{-15}
	0.003	8.2×10^{-6}	5.2×10^{-6}	3.1×10^{-6}	1.7×10^{-6}	2.0×10^{-14}
	0.004	1.0×10^{-5}	6.4×10^{-6}	3.9×10^{-6}	2.1×10^{-6}	4.8×10^{-14}
	0.005	1.1×10^{-5}	7.6×10^{-6}	4.6×10^{-6}	2.5×10^{-6}	9.3×10^{-14}
0.4	0.001	5.0×10^{-6}	3.0×10^{-6}	1.7×10^{-6}	9.3×10^{-7}	9.8×10^{-16}
	0.002	8.1×10^{-6}	5.1×10^{-6}	3.0×10^{-6}	1.6×10^{-6}	7.9×10^{-15}
	0.003	1.0×10^{-5}	6.9×10^{-6}	4.1×10^{-6}	2.2×10^{-6}	2.6×10^{-14}
	0.004	1.3×10^{-5}	8.5×10^{-6}	5.2×10^{-6}	2.8×10^{-6}	6.3×10^{-14}
	0.005	1.5×10^{-5}	1.0×10^{-5}	6.2×10^{-6}	3.4×10^{-6}	1.2×10^{-13}
0.5	0.001	6.2×10^{-6}	3.8×10^{-6}	2.2×10^{-6}	1.1×10^{-6}	1.2×10^{-15}
	0.002	1.0×10^{-5}	6.3×10^{-6}	3.8×10^{-6}	2.0×10^{-6}	9.7×10^{-15}
	0.003	1.3×10^{-5}	8.6×10^{-6}	5.2×10^{-6}	2.8×10^{-6}	3.2×10^{-14}
	0.004	1.6×10^{-5}	1.0×10^{-5}	6.4×10^{-6}	3.5×10^{-6}	7.7×10^{-14}
	0.005	1.9×10^{-5}	1.2×10^{-5}	7.6×10^{-6}	4.2×10^{-6}	1.5×10^{-13}

Table 4 shows the numerical solution of the function $w(x,t)$, which was derived from the solution of the CTFCJMS using the CEADM. The table displays the results for various values of x, t, and α.

Table 4. Numerical solution of $w(x,t)$ by CEADM for CTFCJMS with different x, t and α at $\lambda = 0.5$.

x	t	$\alpha = 0.75$	$\alpha = 0.80$	$\alpha = 0.85$	$\alpha = 0.90$	$\alpha = 1$
0.1	0.001	2.5×10^{-6}	1.5×10^{-6}	9.0×10^{-7}	4.7×10^{-7}	3.1×10^{-16}
	0.002	4.1×10^{-6}	2.6×10^{-6}	1.5×10^{-6}	8.3×10^{-7}	2.5×10^{-15}
	0.003	5.5×10^{-6}	3.5×10^{-6}	2.1×10^{-6}	1.1×10^{-6}	8.5×10^{-15}
	0.004	6.8×10^{-6}	4.3×10^{-6}	2.6×10^{-6}	1.4×10^{-6}	2.0×10^{-14}
	0.005	7.9×10^{-6}	5.1×10^{-6}	3.1×10^{-6}	1.7×10^{-6}	3.9×10^{-14}
0.2	0.001	5.0×10^{-6}	3.1×10^{-6}	1.8×10^{-6}	9.4×10^{-7}	6.3×10^{-16}
	0.002	8.3×10^{-6}	5.2×10^{-6}	3.1×10^{-6}	1.6×10^{-6}	5.0×10^{-15}
	0.003	1.1×10^{-5}	7.0×10^{-6}	4.2×10^{-6}	2.3×10^{-6}	1.7×10^{-14}
	0.004	1.3×10^{-5}	8.6×10^{-6}	5.3×10^{-6}	2.9×10^{-6}	4.0×10^{-14}
	0.005	1.5×10^{-5}	1.0×10^{-5}	6.2×10^{-6}	3.4×10^{-6}	7.9×10^{-14}
0.3	0.001	7.5×10^{-6}	4.6×10^{-6}	2.7×10^{-6}	1.4×10^{-6}	9.4×10^{-16}
	0.002	1.2×10^{-5}	7.7×10^{-6}	4.6×10^{-6}	2.4×10^{-6}	7.5×10^{-15}
	0.003	1.6×10^{-5}	1.0×10^{-5}	6.3×10^{-6}	3.4×10^{-6}	2.5×10^{-14}
	0.004	2.0×10^{-5}	1.2×10^{-5}	7.9×10^{-6}	4.3×10^{-6}	6.0×10^{-14}
	0.005	2.3×10^{-5}	1.5×10^{-5}	9.3×10^{-6}	5.1×10^{-6}	1.1×10^{-13}
0.4	0.001	1.0×10^{-5}	6.1×10^{-6}	3.5×10^{-6}	1.8×10^{-6}	1.2×10^{-15}
	0.002	1.6×10^{-5}	1.0×10^{-5}	6.1×10^{-6}	3.3×10^{-6}	9.9×10^{-15}
	0.003	2.1×10^{-5}	1.3×10^{-5}	8.4×10^{-6}	4.5×10^{-6}	3.3×10^{-14}
	0.004	2.6×10^{-5}	1.7×10^{-5}	1.0×10^{-5}	5.7×10^{-6}	7.9×10^{-14}
	0.005	3.1×10^{-5}	2.0×10^{-5}	1.2×10^{-5}	6.8×10^{-6}	1.5×10^{-13}
0.5	0.001	1.2×10^{-5}	7.6×10^{-6}	4.4×10^{-6}	2.3×10^{-6}	1.5×10^{-15}
	0.002	2.0×10^{-5}	1.2×10^{-5}	7.6×10^{-5}	4.1×10^{-6}	1.2×10^{-14}
	0.003	2.7×10^{-5}	1.7×10^{-5}	1.0×10^{-5}	5.7×10^{-6}	4.1×10^{-14}
	0.004	3.3×10^{-5}	2.1×10^{-5}	1.3×10^{-5}	7.1×10^{-6}	9.8×10^{-14}
	0.005	3.8×10^{-5}	2.5×10^{-5}	1.5×10^{-5}	8.5×10^{-6}	1.9×10^{-13}

4. DISCUSSION AND CONCLUSION

Figure 1 displays the three-dimensional graphs of the numerical solutions obtained by the Cq-HATM, as well as the exact solutions and the absolute errors between the Cq-HATM solutions and the exact solutions for the CTFCJMS. The three-dimensional graphs depicting the numerical solutions obtained by the CEADM for the CTFCJMS are shown in Figure 2. Additionally, the exact solutions and the absolute errors between the CEADM solutions and the exact solutions are also illustrated in the same figure. Figure 3 depicts the two-dimensional graphs of the solutions $u(x,t)$ and $w(x,t)$ of the CTFCJMS, obtained using the Cq-HATM, for various alpha values. The two-dimensional graphical representations of the solutions $u(x,t)$ and $w(x,t)$ of the CTFCJMS are shown in Figure 4, which have been derived by the utilization of the CEADM, while considering different values of α. The numerical solutions of $u(x,t)$ and $w(x,t)$ found using Cq-HATM for the values of $\alpha = 0.75, \alpha = 0.8, \alpha = 0.85, \alpha = 0.9$, and $\alpha = 1$ for CTFCJMS are presented in Tables 1-2. Also, the numerical solutions of $u(x,t)$ and $w(x,t)$ found using CEADM for various values of $\alpha = 0.75, \alpha = 0.8, \alpha = 0.85, \alpha = 0.9$, and $\alpha = 1$ for CTFCJMS are presented in Tables 3-4.

In this study, CTFCJMS has been examined by the new numerical methods, namely, Cq-HATM and CEADM. The reliability of these new methods has been confirmed by numerical results. The new methods presented to solve such coupled fractional systems have been determined to possess notable advantages and demonstrate effectiveness.

CONFLICT OF INTEREST

The authors stated that there are no conflicts of interest regarding the publication of this article.

AUTHORSHIP CONTRIBUTIONS

Autors' contributions are equal.

REFERENCES

[1] Liouville J. 1832. Mémoire sur quelques questions de géométrie et de mécanique, et sur un nouveau genre de calcul pour résoudre ces questions. J Ecole Polytech 1832; 13(21): 1-69.

[2] Miller KS, Ross B. An introduction to the fractional calculus and fractional differential equations. Wiley, New York, 1993.

[3] Podlubny I. Fractional Differential Equations. Academic Press, New York, 1999.

[4] Baleanu D, Diethelm K, Scalas E, Trujillo JJ. Fractional calculus: models and numerical methods. World Scientific, London, 2012.

[5] Povstenko Y. 2015. Linear fractional diffusion-wave equation for scientists and engineers. Birkhäuser, Switzerland, 2015.

[6] Baleanu D, Wu GC, Zeng SD. Chaos analysis and asymptotic stability of generalized Caputo fractional differential equations. Chaos Solit Fractals 2017; 102: 99–105.

[7] Sweilam NH, Abou Hasan MM, Baleanu D. New studies for general fractional financial models of awareness and trial advertising decisions. Chaos Solit Fractals 2017; 104: 772-784.

[8] Liu DY, Gibaru O, Perruquetti W, Laleg-Kirati TM. Fractional order differentiation by integration and error analysis in noisy environment. IEEE Trans Automat 2015; 60: 2945–2960.

[9] Esen A, Sulaiman TA, Bulut H, Baskonus HM. Optical solitons to the space-time fractional (1+1)-dimensional coupled nonlinear Schrödinger equation. Optik 2018; 167: 150–156.

[10] Caponetto R, Dongola G, Fortuna L, Gallo A. New results on the synthesis of FO-PID controllers. Commun Nonlinear Sci Numer Simul 2010; 15: 997–1007.

[11] Veeresha P, Prakasha DG, Baskonus HM. Novel simulations to the time-fractional Fisher's equation. Math Sci 2019; 13(1): 33-42.

[12] Khalil R, Al Horani M, Yousef A, Sababheh M. A new definition of fractional derivative. J Comput Appl Math 2014; 264: 65-70.

[13] Aggarwal S, Chauhan R, Sharma N. 2018. Application of Elzaki transform for solving linear Volterra integral equations of first kind. Int J Res Advent Technol 2018; 6(12): 3687-3692.

[14] Elzaki TM. Applications of new transform "Elzaki transform" to partial differential equations. Glob J Pure Appl Math 2011; 7(1): 65-70.

[15] Elzaki TM. Solution of nonlinear differential equations using mixture of Elzaki transform and differential transform method. In International Mathematical Forum, 2012; 7(13): 631-638.

[16] Elzaki TM, Hilal EMA. Homotopy perturbation and Elzaki transform for solving nonlinear partial differential equations. Math Theory Model 2012; 2(3): 33-42.

[17] Elzaki TM, Kim H. The solution of radial diffusivity and shock wave equations by Elzaki variational iteration method. Int J Math Anal 2015; 9(22): 1065-1071.

[18] Jena RM, Chakraverty S. Solving time-fractional Navier–Stokes equations using homotopy perturbation Elzaki transform. SN Appl Sci 2019; 1: 1-16.

[19] Abu-Gdairi R, Al-Smadi M, Gumah G. An expansion iterative technique for handling fractional differential equations using fractional power series scheme. J Math Stat 2015; 11(2), 29–38.

[20] Baleanu D, Golmankhaneh AK, Baleanu MC. Fractional electromagnetic equations using fractional forms. Int J Theor Phys 2009; 48(11): 3114–3123.

[21] Baleanu D, Jajarmi A, Hajipour M. On the nonlinear dynamical systems within the generalized fractional derivatives with Mittag–Leffler kernel. Nonlinear Dyn 2018; 2018(1): 1–18.

[22] Baleanu, D., Asad, J. H., Jajarmi, A. 2018. New aspects of the motion of a particle in a circular cavity. Proc Rom Acad Ser A, 2018; 19(2): 143–149.

[23] Baleanu D, Jajarmi A, Bonyah E, Hajipour M. New aspects of poor nutrition in the life cycle within the fractional calculus. Adv Differ Equ 2018; 2018(1): 1-14.

[24] Anaç H, Merdan M, Bekiryazıcı Z, Kesemen T. Bazı Rastgele Kısmi Diferansiyel Denklemlerin Diferansiyel Dönüşüm Metodu ve Laplace-Padé Metodu Kullanarak Çözümü. Gümüşhane Üniversitesi Fen Bilimleri Enstitüsü Dergisi 2019; 9(1): 108-118.

[25] Ayaz F. Solutions of the system of differential equations by differential transform method. Appl Math Comput 2004; 147(2): 547-567.

[26] He JH. Variational iteration method-a kind of non-linear analytical technique: some examples. Int J Non Linear Mech 1999; 34(4): 699-708.

[27] He JH. Homotopy perturbation method: a new nonlinear analytical technique. Appl Math Comput 2003; 135(1): 73-79.

[28] He JH. Homotopy perturbation method for solving boundary value problems. Phys Lett 2006; 350(1-2): 87-88.

[29] He JH. Addendum: new interpretation of homotopy perturbation method. Int J Mod Phys B 2006; 20(18): 2561-2568.

[30] Jajarmi A, Baleanu D. Suboptimal control of fractional-order dynamic systems with delay argument. J Vib Control 2018; 24(12): 2430-2446.

[31] Jajarmi A, Baleanu D. A new fractional analysis on the interaction of HIV with CD4+ T-cells. Chaos Solitons Fractals 2018; 113: 221-229.

[32] Kangalgil F, Ayaz F. Solitary wave solutions for the KdV and mKdV equations by differential transform method. Chaos Solitons Fractals 2009; 41(1): 464-472.

[33] Klimek M. Fractional sequential mechanics-models with symmetric fractional derivative. Czech J Phys 2001; 51(12): 1348-1354.

[34] Merdan M. A new applicaiton of modified differential transformation method for modeling the pollution of a system of lakes. Selçuk J Appl Math 2010; 11(2): 27-40.

[35] Alkan A. Improving homotopy analysis method with an optimal parameter for time-fractional Burgers equation. Karamanoğlu Mehmetbey Üniversitesi Mühendislik ve Doğa Bilimleri Dergisi, 2022; 4(2): 117-134.

[36] Wang K, Liu S. A new Sumudu transform iterative method for time-fractional Cauchy reaction-diffusion equation. Springer Plus 2016; 5(1): 865.

[37] Wazwaz AM. A reliable modification of Adomian decomposition method. Appl Math Comput 1999; 102(1): 77-86.

[38] Aslefallah M, Abbasbandy S, Yüzbaşi Ş. (2023). Numerical Solution for a Class of Nonlinear Emden-Fowler Equations by Exponential Collocation Method. Appl Appl Math 2023; 18(1): 1-13.

[39] Abdeljawad, T. 2015. On conformable fractional calculus. J Comput Appl Math 2015; 279: 57-66.

[40] Ala V, Demirbilek U, Mamedov KR. An application of improved Bernoulli sub-equation function method to the nonlinear conformable time-fractional SRLW equation. AIMS Math 2020; 5(4): 3751-3761.

[41] Gözütok U, Çoban H, Sağıroğlu Y. Frenet frame with respect to conformable derivative. Filomat 2019; 33(6): 1541-1550.

[42] Shrinath M, Bhadane A. New conformable fractional Elzaki transformation: Theory and applications. Malaya J Mat 2019; 1: 619-625.

[43] Kaya D, El-Sayed SM. A numerical method for solving Jaulent-Miodek equation. Phys Lett A, 2003; 318(4-5): 345-353.

[44] Cinar M, Onder I, Secer A, Bayram M, Abdulkadir Sulaiman T, Yusuf A. Solving the fractional Jaulent–Miodek system via a modified Laplace decomposition method. Waves Random Complex Media 2022; 1-14.

[45] Silva FS, Moreira DM, Moret MA. Conformable Laplace transform of fractional differential equations. Axioms, 2018; 7(3): 55.